Seismic zones regionalization and hazard assessment of SW Arabian Shield and Southern Red Sea Region

16

M. A. Al-Malki and A. M. Al-Amri

Introduction

The study area located between Lat. 14°–19°N and Long. 39°–45°E including southwestern part of Saudi Arabia, Northern Yemen and the southern part of the Red Sea (Fig. 16.1). It is characterized by a various topographic features as plateaux of Hejaz and Asir (1300–2000 m above Sea level) extends along the western coast of Saudi Arabia. The Northern Yemen has a complicated topographic regions as; (1) coastal plain region, extends along the coast of Yemen; (2) mountain highs region extends from the northern to southern Yemen borders; (3) mountain basins region that includes the main basins and plains within the mountain highs (e.g. Yarim, Dhamar, Sadah) and finally plateau belt which present in the east and north of mountain highs region. The Red Sea can be divided into three physiographic regions; the narrow continental margins, the main trough and the deep axial trough (Drake and Girdler 1964). South of Latitude 24°N, a deep axial trough appears in the main trough.

The importance of conducting this study is related primarily to the study area as follows; (1) The area has a new urban communities and big cities with heavy populations, (2) The area is promising with many strategic and developmental projects, (3) its buildings don't follow the seismic design regulations although it is affected by many destructive earthquakes (e.g. 1982 Yemen earthquake), (4) its complicated structural and tectonic setting. So, it is necessary to assess its seismic hazard potentialities in terms of Peak Ground Acceleration (PGA) and the site response characteristics at big cities lie within this area to mitigate the direct impact of earthquakes on the human life and buildings within the area.

The previous studies showed that the Arabian plate subjected to the tectonic movements since Pliocene age, where great lateral movements started to move the continental blocks toward the north (40 km) of the Arabian plate with relative to the African plate and formed narrow strait of Bab El-Mandeb (Abdel-Gawad 1969). These movements continued to the northeastern direction along the Gulf of Aqaba (150 km) (Freund et al. 1970) in the Middle Miocene age. Left-Lateral movement (40–45 km) for the Miocene rocks in Sinai area and led to the formation of the axial trough of the Red Sea. The spreading rate was asymmetric during these movements along the Red Sea as indicated from the change in the width of the axial trough. As a result of these movements a more complicated structures were formed including major faults in the south of Saudi Arabia and causing many earthquakes. Depending on the geological, geophysical studies as well as the distribution of recent earthquakes in the Red Sea and comparison with the location of earthquakes in Tahoma and Arabian Shield, it is noticed that there is a possibility for the extension of some faults from offshore into the land especially between 16.3° and 17.4°N to the northeastern of Abha and it is considered that these faults are responsible for the western Abha earthquake 1,408 H (5.2 magnitude). The northeastern faults were formed due to separation of Arabian plate from Nubian plate in the northeastern direction. Based on the Heat Flow Density (HFD) studies (Makris et al. 1986, 1989), the type of crust can be differentiated.

From the historical and instrumental earthquake studies (Al-Amri 1994) it is noticed that most of earthquakes have occurred along the axial trough of the Red Sea. But there are four earthquakes in 1941 (Mb = 6.25), 1955 (Mb = 5.7), 1962 (Ms = 4.7) and 1982 (Mb = 6) have occurred away from the axial trough of Red Sea (Langer et al. 1987). Some seismic hazard studies (Barazangi 1981 and Thenhaus 1983) carried out for the southern Red Sea based on the probabilistic approach. Al-Amri (1995)

M. A. Al-Malki (✉)
King Abdulaziz City for Science and Technology, 6086 Riyadh 11442, Saudi Arabia
e-mail: malmalki@kacst.edu.sa

A. M. Al-Amri
Department of Geology, King Saud University, 2455 Riyadh 11451, Saudi Arabia

K. Al Hosani et al. (eds.), *Lithosphere Dynamics and Sedimentary Basins: The Arabian Plate and Analogues*, Frontiers in Earth Sciences,
DOI: 10.1007/978-3-642-30609-9_16,

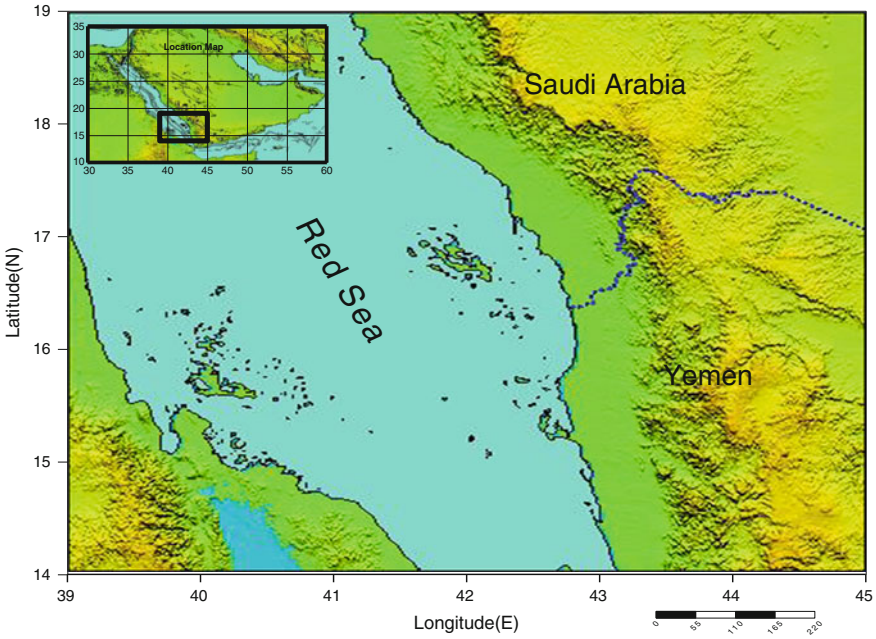

Fig. 16.1 Location and topographical features of the study area

divided the southern Red Sea into two main seismic source zones.

Geologic Setting

The structural pattern of the eastern Arabian region (Powers et al. 1966) was set in Precambrian time with stabilization of the Arabo-Nubian shield. The igneous and metamorphic rocks constitute the main part of the Arabian Shield. The age of Arabian Shield ranges from 1,000 to 450 Ma. This shield covers a vast surface area of the study area including southern Saudi Arabia and Yemen. The Arabian Shield rocks represent communities of many Arc Islands with some residuals of oceanic crust (Ophiolite) that gathered due to collision for 900 to 650 my. The thickness of crust is increased by magmatic activity (Brown et al. 1963). This shield is divided into intraoceanic island–Arc terrains (hijaz and Asir). These terranes are separated by suture zones of two types, island Arc-island Arc collisional sutures and island Arc—Continental collisional sutures. Nabitah orogenic belt is of second type and is the longest and most prominent, dividing the exposed shield in the middle. The western sutures are NE trending while the eastern ones are N–S trending. These Arabian Shield rocks are overlaid by sedimentary rocks of Cambrian to recent (Fig. 16.2).

In Late Tertiary the great rift-fault systems of Africa and Red Sea also began to take on their present form, although movement on these faults may have started somewhat earlier. The Red Sea was developed by three tectonic movements led to formation of the southern part, northern part and Red Sea itself. The southern part the Red Sea is connected to the Gulf of Aden, which trends ENE–WSW, in Afar area where injected magma upward from the upper mantle and led to the formation of the regional joints in this part within 20 to 30 my.

Seismic Hazard Assessment

Seismicity of the Area

The study area is affected by about 538 earthquakes with magnitude ranges from 2.4 to 6.9 during the period from 200 to 2005 A.D. This earthquake activity can be divided into two types;

Historical Seismicity (200–1964)

According to the research in the published compilations of historical earthquakes for the Middle East (Poirier and Taher 1980; Al sinawi 1983, 1986; Ambraseys and Mellvile 1983; Ambraseys et al. 1994), the historical seismicity is of the swarm-type and some of these events were related to the volcanic eruptions. There are about 78 earthquakes have occurred in the area of study in the period from 200 to 1900 (Fig. 16.3) and revealed that; (1) most of earthquakes are concentrated around Sana'a—Aden along the Red Sea; (2) Some of the historical earthquakes have occurred on offshore and these earthquakes were felt on the land. There are about 22 earthquakes have occurred in the period from 1900 till 1964 with magnitude ranges between 4 and 6.3; (3) Most of historical earthquakes seem to correlate with the general tectonics of the region (El-Isa and Al-Shanti 1989). A major

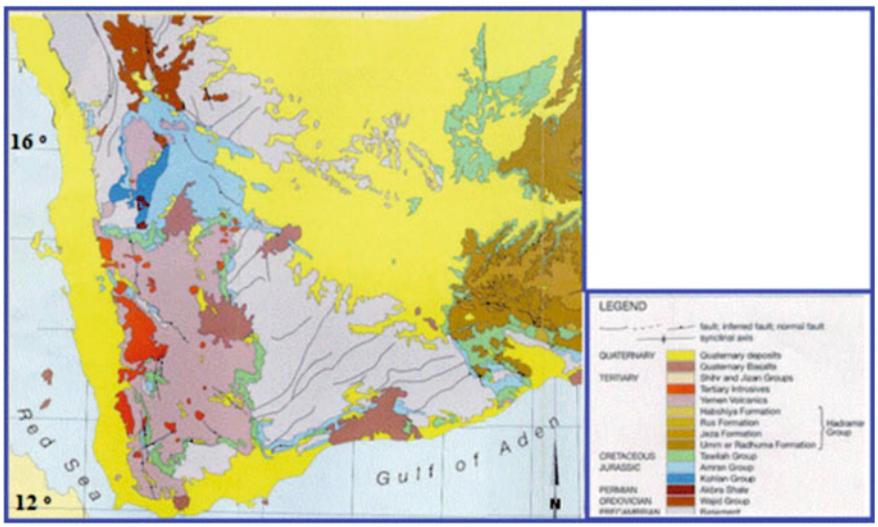

Fig. 16.2 Surface geological units of study area

characteristic of the epicenters is a NW alignment, parallel to the axis of the Red Sea where some instrumental earthquakes occur as well. A perpendicular alignment is also observed.

Instrumental Seismicity (1964–2005)

The instrumental earthquakes are collected from a number of seismological catalogues and bulletins including those of the International Seismological Centre (ISC), National Earthquake Information Service (NIES), El-Isa and Al-Shanti (1989) and Al-Amri (1994) and Saudi Geological Survey (SGS). It is found that about 438 earthquakes are occurred study area within the period 1964–2005 with magnitudes in the range $2 \leq mb \leq 6.9$. The local earthquake monitoring in Saudi Arabia stated in 1964 with few stations and then the number of stations has been increased. One hundred Forty-eight of these had a magnitude $M \geq 4$, while the rest has magnitude less than 4. The epicentral distribution of the instrumental seismicity of the study area (Fig. 16.4) shows the following characteristics; (1) the general distribution of earthquakes seems to correlate well with the major structures of the area. Many earthquakes are distributed within the spreading zone of the Red Sea. South of Sanaa a concentration of epicenters correlates well with a regional Tertiary and Quaternary volcanic plateau; (2) the instrumental earthquakes show a noticeable higher activity in the southern Red Sea and Middle of the Red Sea compared with other areas.

Identification of Seismic Source Zones

The definition of a seismic source zone is based—to large extent- on the interpretation of the geological, geophysical and seismological data. Thenhaus (1983) noted that the procedures used in delineating the seismic source zones are

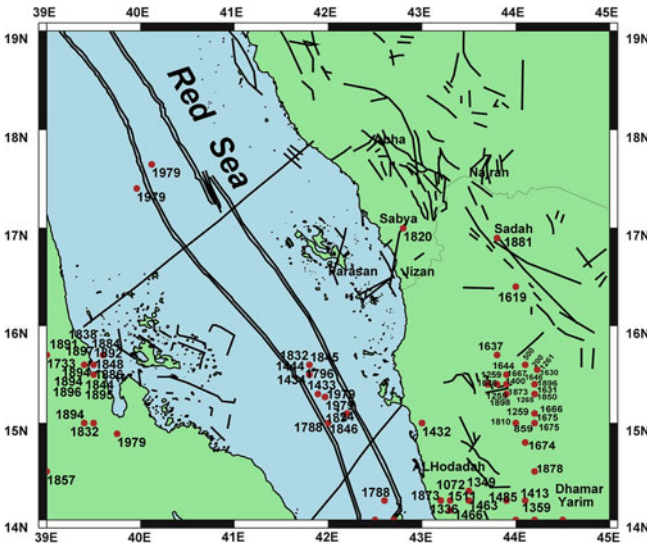

Fig. 16.3 Historical seismicity within the area of study

ill defined. Seismic zones delineation is important not only for theoretical reasons (improvement of understanding the geodynamics of a region, etc.) but also for practical reasons.

The definition of seismic zones carried out in the present work depends on both of historical and instrumental earthquakes as well as the results of the previous geophysical and geological studies including the kind of seismic faulting (Papazachos et al. 1984), seismicity rate (a & b values, Papazachos 1980 and Hatzidimitriou et al. 1985), major trends of geological zones (Mountrakis et al. 1983), and the fault plane solutions of the major earthquakes (strike, dip and stress axes) (Al-Amri and Al-Khalifa 2004). A seismic zone is a configuration within which it is assumed that an earthquake recurrence process is considered to be spatially and temporally homogeneous. The delineation of the seismotectonic sources is usually represents the major

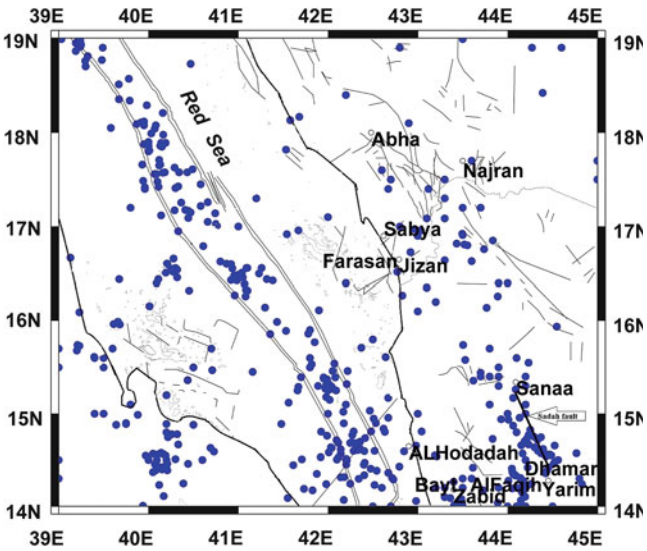

Fig. 16.4 Distribution of instrumental earthquakes within the area

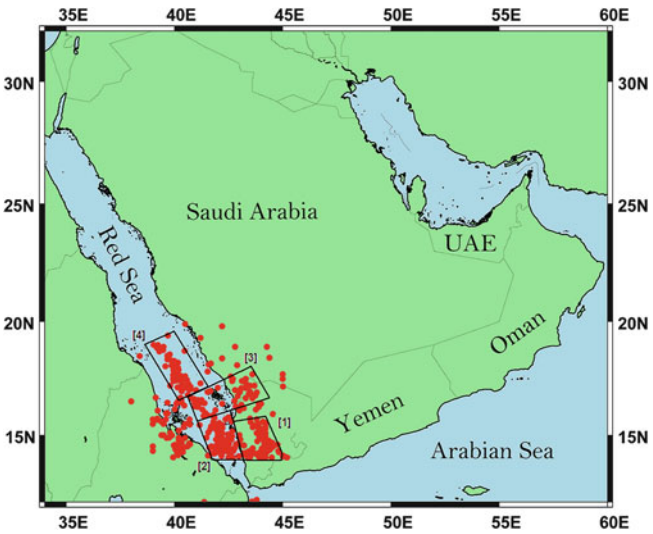

Fig. 16.5 Delineated seismic source zones

part of any seismic hazard analysis. According to this study the seismic activities are concentrated in four narrow belts (Fig. 16.5) and these belts are:

1. Sana'a–Dhamar (southern Arabian Shield) zone.
2. Southern Red Sea zone.
3. Northern Yemen zone.
4. Middle Red Sea zone.

1. Sana'a–Dhamar (southern Arabian Shield) zone

This zone includes the Sadah active fault which characterized by its higher seismic activity. The strongest earthquake that occurred in this zone is December 12, 1982 earthquake (Ms = 6.1). The fault plane solution of this earthquake indicates normal fault. There are many destructive earthquakes and swarms have occurred in this zone (Ambraseys 1988 and Al-Amri 1998).

2. Southern Red Sea zone

This zone includes many earthquakes occurred in the southern Red Sea. This zone characterized by high rate of seismic slip and this due to presence of this zone near to the triple junction point between east African Rift system, Gulf of Aden and the Red Sea. The Heat Flow studies also indicate that there is a high rate of Heat Flow Density (HFD) due to igneous magmatic intrusions in this seismic zone. The maximum observed earthquake magnitude in this zone is 6.9 (Al-Amri and Al-Khalifa 2004). From the fault plane solution of earthquakes in this zone indicate that about 75 % of earthquakes were occurred along the normal faults (Dhamar area) while, 25 % were strike-slip fault (Zabid area).

3. Northern Yemen zone

This zone includes the earthquakes located in the axial trough and the main trough of the Red Sea. It is noticed that there are two types of faults prominent in the Red Sea; the Red Sea Axial Rift Spreading System of faults and the other is the transform faults. It is concluded that the seismic activity in this zone is related to the transform faults accompanied with the tensional movements. But the seismic activity of this zone in the mainland is related to isolated tectonic structures where the strongest earthquake in this zone was in January 11, 1941 (Ms = 6.2).

4. Middle of Red Sea zone

This zone includes the seismic activity extends along the axial trough of the Red Sea which is characterized by high rate of Heat Flow Density and Bouguer anomalies (Al-Amri 1994 and 1998). From the earthquakes that occurred in this zone, the 1967 earthquake (Mb = 6.7) with strike-slip fault (Fairhead, 1968; McKenze, Davis and Molnar 1970; Fairhead and Girdler 1970 and Fairhead and Girdler 1972).

Determination of a- & b-Values

The seismicity of an area can be defined as a function of the size of the earthquakes (magnitude, seismic moment, etc.) and of the frequency of the occurrence of these earthquakes. The basic law, which is applied for determination of the seismicity of an area, is the well-known frequency-magnitude statistical relation (Gutenberg and Richter 1944). But there are some conditions to apply this relation for the determination of the seismicity in an area; the area must be seismotectonically homogeneous (constant value of the b parameter of the frequency-magnitude relation, etc.). For this reason, it is necessary to separate the whole study region into seismic zones, which should be as much as possible seismotectonically homogeneous.

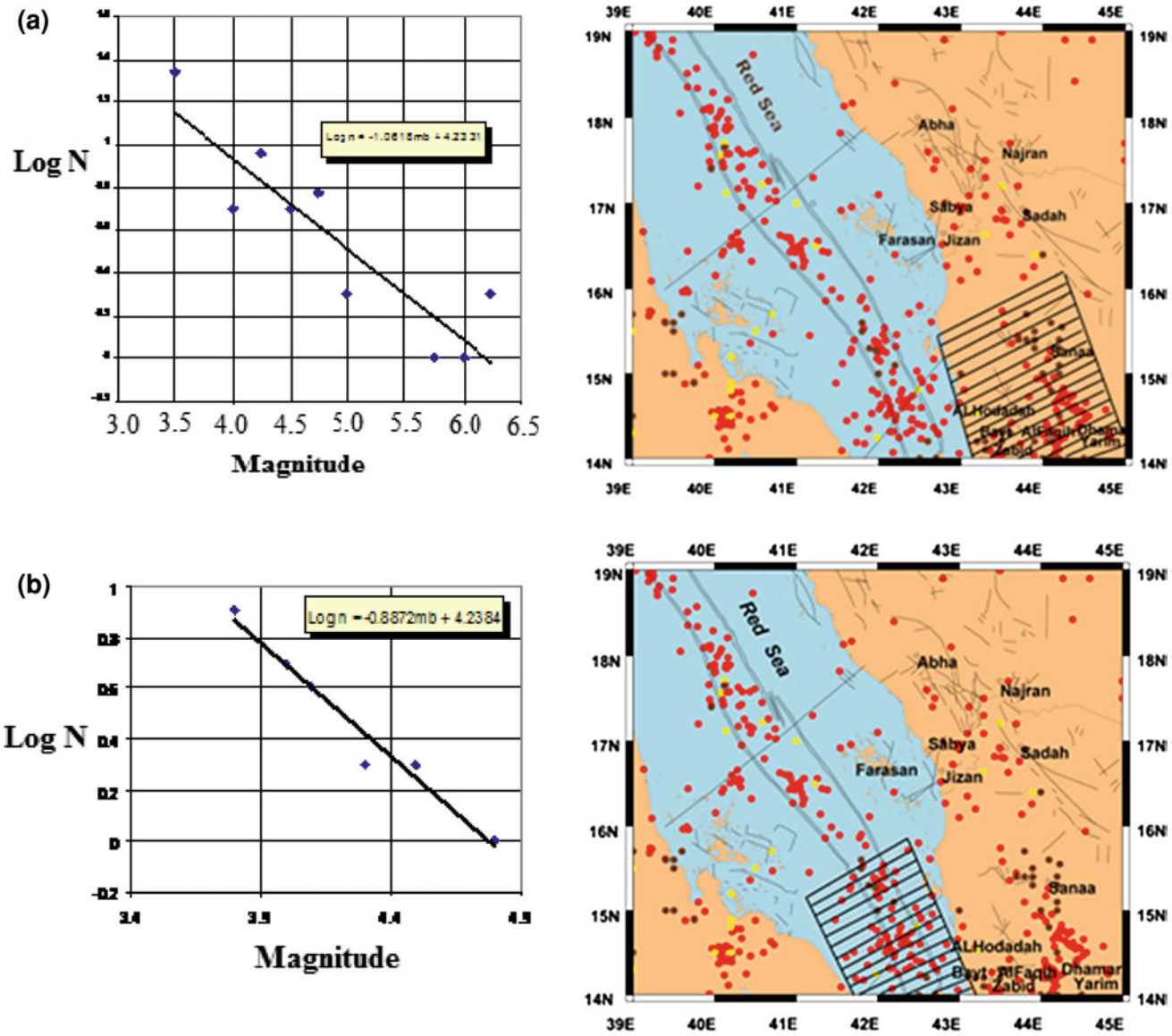

Fig. 16.6 **a** Gutenberg-Richter relation for zone *1* **b** Gutenberg-Richter relation for zone *2* **c** Gutenberg-Richter relation for zone *3* **d** Gutenberg-Richter relation for zone *4*

For each seismic source, the magnitude distribution was taken to be exponential and of the form given by the Richter relation of occurrence frequencies:

$$\log N = a - bM \tag{16.1}$$

Where N: is the number of earthquakes of magnitude ≥M, a & b are constants, and the logarithms are taken to the base 10. The value of "a" depends on the period of observation, the size of the region considered and the level of seismic activity, whereas "b- value" depends on the ratio of the number of strong and weak earthquakes. The values of "b" have been reported to differ from 0.5 to 1.5 approximately and mostly between 0.7 and 1.0 (Isacks and Oliver 1964). Nevertheless, many researchers believe that "b" varies from region to region and also varies with the focal depth. Besides, its value depends on the stress conditions and on the heterogeneity of the rock volume generating the earthquakes (Mogi 1962 and Karnik 1969).

In the study area it is found that, some of the seismic source zones have a small number of earthquakes and also preclude direct assessment of a-values for individual zones. Hence, a regional rate of earthquake activity was calculated for whole area of study by summing all the activity in all the seismic source zones. This regional rate of activity was then apportioned among the individual source zones so that the amount of activity applied to each zone reflects the number

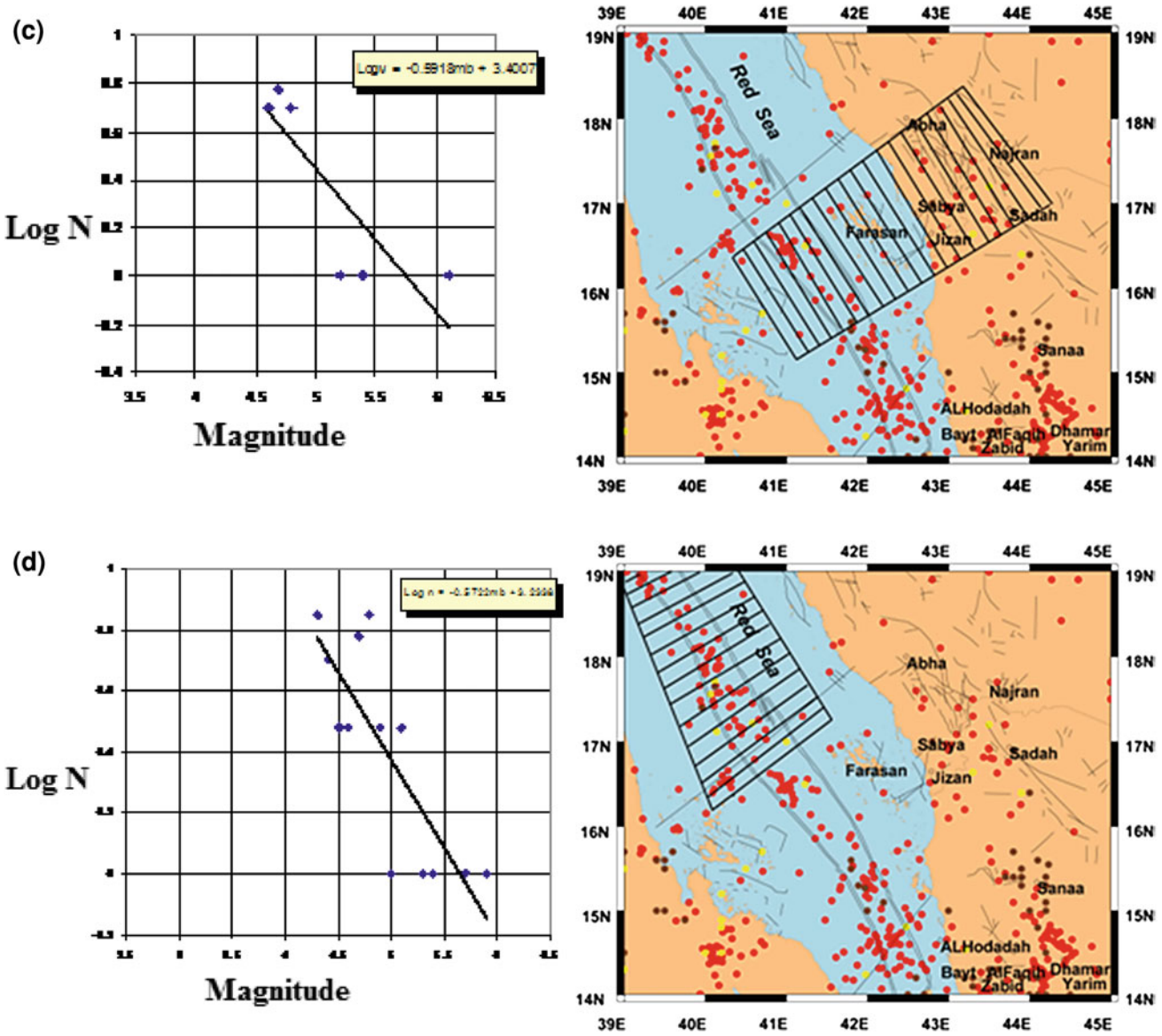

Fig. 16.6 (continued)

of earthquake events occurring in that zone. The magnitude–Frequency relations for different tectonic units are calculated (Fig. 16.6 and Table 16.1) using least squares fitting between log N and M.

According to Fig. 16.6; it can noticed that:

- The zones of moderate seismic activity (zones 1 and 2) are characterized by moderate slopes (0.88–1.06) which correlate with tensional forces under these zones. While the lowest slopes (lowest "b" ranging from 0.57 to 0.59) correspond to the zones of lesser seismic activity (zones 3 and 4) and this may also indicate the scarcity of strong earthquakes in this tectonic unit.
- It is possible to correlate between the slopes "b" and the stage of tectonic development for the tectonic province of southern Red Sea, that the "b" values increase to the south in the direction of the Red Sea opening.

Determination of the Maximum Expected Magnitude (Mw max.)

This step requires a determination of the maximum earthquake for each of the identified seismotectonic sources. In the d eterministic analyses, it is more common to define the maximum earthquake as a maximum credible earthquake. This earthquake is based upon an evaluation of those processes, which are reasonably expected to be associated with

Table 16.1 Parameters of defined seismic source zones

Seismic zone	No. of earthquakes	a-value	b-value
1	48	4.233	1.061
2	87	4.238	0.887
3	51	3.4	0.591
4	77	3.2	0.572

Table 16.2 Maximum expected magnitude for each zone

Zone no.	M_{max}
1	6.6
2	7.4
3	6.7
4	7.2

an earthquake source. Therefore, the maximum expectable or maximum probable earthquake is sometimes used in place of maximum credible (Reiter 1991). Another kind of maximum earthquake is the maximum historic earthquake. The maximum historic earthquake often defines the lower bounds of maximum credible events. If an earthquake struck in the past, then it is certainly credible that it may strike in the future. The instrumental and historical records of earthquake activity, which are often too short to reflect the full potential of faults, may be extended back thousands of years or more to obtain estimates of maximum earthquake occurrence during the past and present tectonic regimes.

Some of the regression relationships are constructed regarding certain issues on their use as follows;

1. Source ruptures length. It is the most frequently employed relationship. Papazachos et al. (2004) defined an empirical relationship between the seismic moment and the rupture length of the fault as:

$$\log(L) = 0.50M_w - 1.86 \qquad (16.2)$$

Where M_w is the moment magnitude and L is the rupture length. To determine the maximum earthquake size that could be generated from the fault, the length of the fault or fault zone is measured and assume that some fixed maximum fraction would rupture in a single earthquake. Along San Andreas this fraction is one-third to two-fifth of the fault total length. Here, this portion is taken to be two-fifth of the total fault length to ensure the conservatism of the results.

Another approach has been adopted to use the historical record by increasing the maximum historical earthquake by arbitrary certain amount and assumes that this value is the appropriate maximum earthquake. This increasing increment is usually taken to be 0.5. This technique is used for some zones for which the fault information is absent. The source rupture length and the maximum historic earthquake on the fault with some increment above it are used to determine the maximum earthquake at each zone within the area of study (Table 16.2).

Simulation of Ground Motion Using Stochastic Method

The stochastic simulation method (Boore 2002) is applied in the area under study in order to predict the ground motion of earthquakes and for the assessment of seismic hazard in terms of Peak Ground Acceleration (PGA) and site response spectra.

Outlines of the Method

The ground motion prediction is based upon the stochastic model, in which ground motion is modeled as band-limited Gaussian noise; the method assumes evenly distributed radiated energy over a specified duration. The method begins with the specification of the Fourier amplitude spectrum of ground acceleration as a function of seismic moment and distance, Y (Mo, R, f), represented by:

$$\mathbf{Y}(\mathbf{Mo}, \mathbf{R}, \mathbf{f}) = \mathbf{E}(\mathbf{Mo}, \mathbf{f})\,\mathbf{P}(\mathbf{R}, \mathbf{f})\,\mathbf{G}(\mathbf{f})\,\mathbf{I}(\mathbf{f}) \qquad (16.3)$$

where E (Mo, f) is the earthquake source spectrum for a specific seismic moment (i.e., Fourier spectrum of the ground acceleration at a distance of 1 km) and P(R, f) is the path effect that models the geometric spreading and the anelastic attenuation of the spectrum as a function of hypocentral distance (R) and frequency (f), G(f) is the site effect and I(f) is a filter used to shape the spectrum to

Table 16.3 Source parameters of the effective earthquakes in each zone

Zone	$\Delta\sigma$	MB (MAX)	Depth (KM)	Density (ρ)	VP	Shear Wave (β)
Z1	30	6.6	9.7	2.85	6.8	3.95
Z2	30	7.4	45	3.2	7.9	4.59
Z3	30	6.7	41	3.2	7.9	4.59
Z4	30	7.2	32.1	3.2	7.9	4.59

correspond to the particular ground motion measure of interest. The time domain implementation of the stochastic method used in this study begins with the generation of a windowed acceleration time series comprised of random Gaussian noise with zero mean amplitude and variance chosen to give unit spectral amplitude on the average. The duration of the window is chosen as a function of magnitude and distance. The spectrum of the windowed time series is multiplied by the desired spectrum [Y(Mo, R, f) from Eq. (16.3)]. The filtered spectrum is then transformed back into the time domain to yield a simulated record for that magnitude and distance.

Input Parameters

These include all the terms of Eq. (16.3) and the duration of motion. The simulations will apply to the random horizontal component of the shear phase of ground motion.

1. The source parameters **[E (Mo, f)]**

The earthquake source spectrum E (Mo, f) for the horizontal component of ground motion is given by the following:

$$\mathbf{E(Mo,\,f)\;=\;C(2\pi f)^2MoS(Mo,f)} \qquad (16.4)$$

where S(Mo, f) is the displacement source spectrum and C is a constant. $C = RsVF/(4\pi\rho\beta 3R)$, with $R = 1$ km, $Rs =$ average shear wave radiation pattern ($= 0.55$), $F =$ free surface effect ($= 2.0$), $V =$ partition onto two horizontal components ($= 0.71$), $\rho =$ the density at the source and β is the shear wave velocity at the source (Table 16.3). In this study the value of stress drop ($\Delta\sigma$) was taken as 30 bar (world-wide average value), where digital data is not available and the estimation of stress drop is difficult.

Where, $\Delta\sigma$ is the stress drop (in bar) and β calculated using Al-Amri and Al-Khalifa, (Al-Amri and Alkhalifah 2004) relation.

2. The path (attenuation) effect (P(R,f), duration)

The path effect or the attenuation parameters that affect the spectrum of motion at a particular site are classified into the geometrical spreading and the anelastic attenuation as represented by the quality factor Q (f).

In this study, the three segments geometrical spreading operator of Atkinson and Boore (1995) is used. R^{-1} geometrical spreading is assumed for distance less than 70 km and $R^{0.0}$ for distances from 70 to 130 km and $R^{-0.5}$ for greater distances. Although the Fourier spectrum of ground motion is not dependent on the duration, it is a very important parameter for peak motions decrease with increasing duration. The duration is a function of the path, as well as the source:

$$\mathbf{T\;=\;To\;+\;bR} \qquad (16.5)$$

where, To is the source duration and bR represents the path dependent term that accounts for dispersion. Following Hanks and McGuire (1981), the source duration is related to the corner frequency by:

$$\mathbf{To\;=\;f_c^{-1}} \qquad (16.6)$$

Empirical observations and theoretical simulations suggest that the path-dependent part of the duration can be represented by a connected series of straight-line segments with different slopes. The function of Boore and Atkinson (1987) is used where the path duration is modeled as trilinear, using the transition distances 70 and 130 km for consistency with the attenuation model. The slope is 0.16 for the distance rages between 10 and 70 km, −0.03 for the distance ranges between 70 and 130 km and 0.04 for the distance ranges from 130 to 1,000 km. The slope is assumed to zero for distances less than 10 km.

It is difficult to study the attenuation effect in the western Arabia and this due to the absence of strong motion records and its complicated crustal structure. The propagation of seismic waves from the Arabian Shield into coastal areas is accompanied with low attenuation like Shield zones allover the world (Thenhaus et al. 1986). Hence one of the empirical attenuation relations for other regions can be selected but these regions should be similar in both of crustal structure and seismotectonic environment with the study area. So, the attenuation relations of the eastern coast of the United States (Nuttli and Herrmann 1984) were used due to the similarity of its geological characteristics with the western coast of the Arabian Peninsula and these relations are as follows;

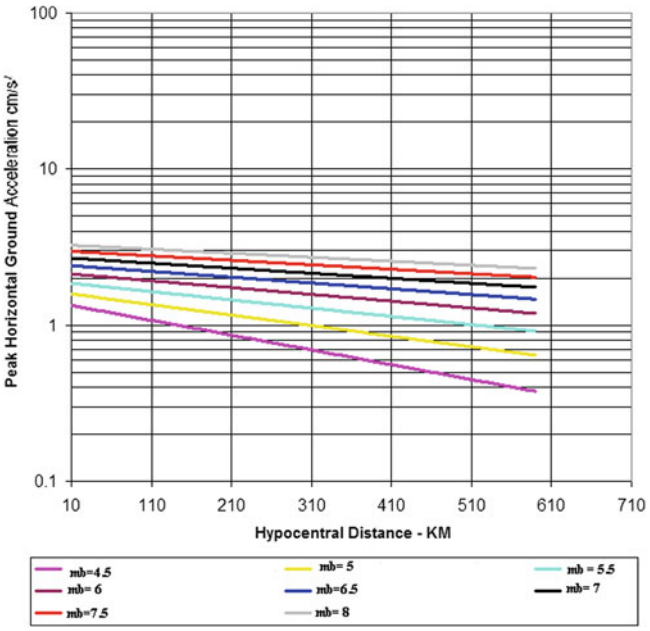

Fig. 16.7 Attenuation curves for peak ground acceleration within the area

$$\mathbf{Log\,A_h = 0.57 + 0.50\,m_b - 0.83\log\left(R^2 + h^2\right)^{1/2} - 0.00069R} \quad (16.7)$$

$$\mathbf{Log\,V_h = -3.60 + 1.00\,m_b - 0.83\log\left(R^2 + h^2\right)^{1/2} - 0.00033R} \quad (16.8)$$

Where R is the hypocentral distance, h is the focal depth of earthquakes in the area of study, Ah is the horizontal Peak ground Acceleration and V_h is horizontal peak ground velocity. These equations were used to study the behavior of waves in the upper crust and to get the attenuation curves of PGA within the study area (Fig. 16.7). It is concluded that the Arabian Shield has a low attenuation values for selected magnitudes when compared with other side of the Red Sea.

3. Local site effect (G(f))

The site properties (effect) that control the change of the seismic ground motion amplitudes at the earth's surface are amplification and diminution (Boore 2002) as follows:

$$\mathbf{G(f) = A(f) + D(f)} \quad (16.9)$$

Velocity and density model is converted into site amplification A(f), using the square root of the impedance ratio between the source and the surface. For polarized shear waves, the impedance is defined as the product of the shear wave velocity, density and the cosine of the angle of incidence. Several relationships between surface geology and local site amplification have deduced (Table 16.4).

The diminution operator D(f) of Eq. (16.9) accounts for the path independent loss of high frequency in the ground motion. For this high-cut filter, (Boore 1983 and 1996) was used:

$$\mathbf{D(f) = \left[1 + (f/f_{max})^8\right]^{-0.5}} \quad (16.10)$$

where f_{max} is the high-frequency cutoff proposed by Hanks (1982), for a limited data set, a value of $f_{max} = 20$ Hz is assumed, due to the absence of strong motion records in Egypt suitable for such determination and to avoid the vital frequencies from engineering sense (up to 10 Hz).

Data Treatment and Results

The area of interest was divided into grid of points every 0.5° in latitudes and longitudes. The SMSIM-Program was running at each point of this grid for each one of the seismic source zone. So, there are different values of PGA at each point of the grid. The maximum expected magnitude of seismic sources that affect the area was used to estimate the ground motion resulted from each zone. Then the maximum PGA value at each point was taken as the representative value at that point and then these values are contoured into maps of PGA at the bedrock and ground surface (Figs. 16.8 and 16.9).

The maximum peak ground acceleration value at bedrock is resulted also from southern Red Sea seismic source and is found to be 41.1 cm/sec^2. While the lowest value of PGA locates in the northeastern part of the area which may relate to the scarcity of earthquake data in this part. The results of this study are compared with the previous studies (Table 16.5). These studies were based on the probabilistic approach for seismic hazard assessment but the present study depends on the stochastic approach which takes all the contribution parameters of the seismic source, attenuation relation due to path and the local site effects into consideration for hazard assessment so, some results are

Table 16.4 Relation between relative amplification and local geology

Reference	Amplification	Geological unit
El-Difrawy (1996)	6.5	Quaternary and fluvial
Midorikawa (1987)	1	Pre-cambrian rocks
Midorikawa (1987)	1	Cretaceous volcanic rocks
Midorikawa (1987)	1	Jurassic

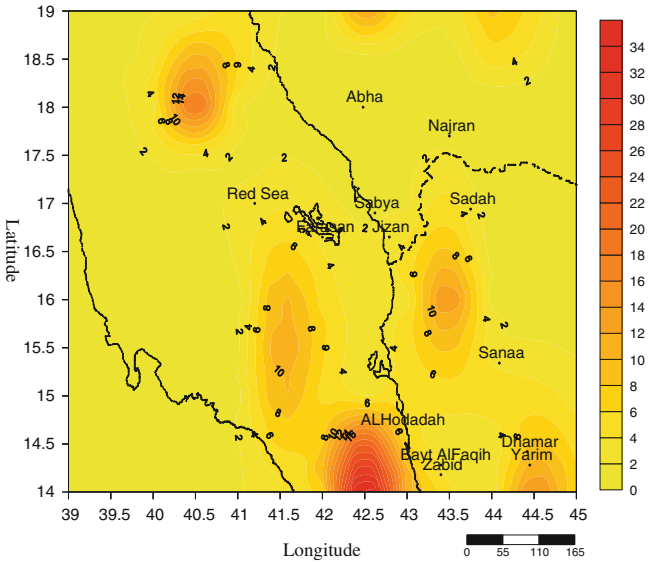

Fig. 16.8 Contour map for values PGA (cm/sec^2) on the bedrock

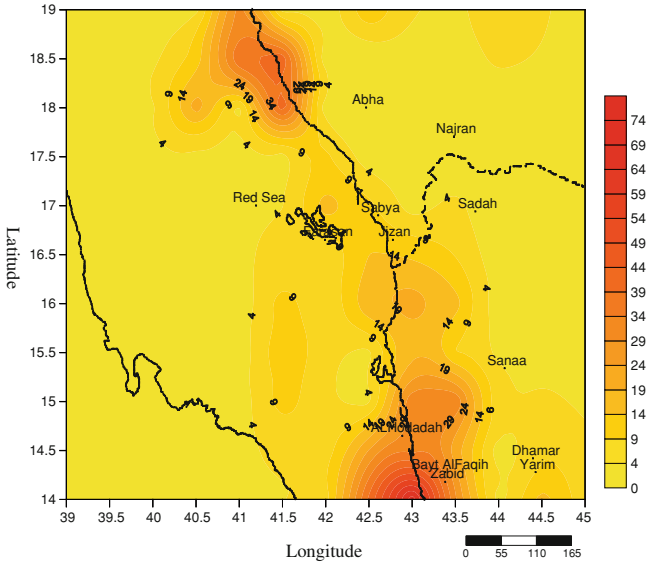

Fig. 16.9 Contour map for values PGA (cm/sec^2) on the ground surface

quite different from the previous studies (Thenhaus et al. 1983; Al-Haddad et al. 1994 and Al-Amri 1995).

While the maximum PGA value at the ground surface reflects the amplification effect of the sedimentary soils at Zabid (32 cm/sec^2), Al-Hodadah (29 cm/sec^2), Farasan (14 cm/sec^2) and Jizan (11.07 cm/sec^2) cities but there is no amplification at other cities. This figure shows that the values of PGA along the Red Sea coast zone are higher than that on the land which reflects the amplification effect of the soft soil along the coast on the PGA values. It is found that the maximum PGA value at the surface is 72.15 cm/sec^2 and resulted also from the southern Red Sea source zone. This indicates that the southern Red Sea area has a great effect on the whole study area.

Response Spectra

Response spectra are defined on the basis of the response of single degree of freedom damped oscillator to the earthquake acceleration. The response spectra of an accelerogram serve the dual function characterizing the ground motion as a function of frequency and provide a tool for determining earthquake resistant design criteria. The response spectra are calculated for four selected damping values at 1, 3, 5 and 10 % of the critical damping for different rock units (Figs. 16.10, 16.11 and 16.12). From Fig. 16.10, it is noticed that the predominant period is 0.1 s. at Quaternary rocks of Sanaa city. The spectral acceleration values are 120, 76, 62 and 46 cm/sec^2 at damping rations 1, 3, 5 and 10 % of critical damping respectively. Also, it is noticed that the spectral curves are attenuated rapidly which reflects the rapidly changes in the behavior of Quaternary sediments under the horizontal forces of earthquakes. Figure 16.11 shows the maximum spectral acceleration value for Tertiary rocks at Dhamar city is 34 cm/sec^2 at damping ratio 1 %, 22 cm/sec^2 at damping ratio 3 %, 18 cm/sec^2 at damping ratio 5 % and 14 cm/sec^2 at damping ratio 10 % of critical damping. The natural period at this site is 0.15 s. Figure 16.12) reflects that the predominant period for Pre-Cambrian rocks at Abha city is 0.25 s. While the spectral acceleration values for damping ratios 1, 3, 5 and 10 % are 1.25, 0.89, 0.75 and 0.55 cm/sec^2 respectively. Also, it is noticed that the spectral curves are broad and attenuated slowly.

Table 16.5 The PGA values from the present study and previous studies

City	Thenhaus et al. (1983) cm/sec^2	AL-Haddad et al. (1994) cm/sec^2	Al-Amri (1995) cm/sec^2	Current study cm/sec^2	
				Bed-rock	Ground surface
Abha	10	15	17	10	10
Jizan	20	20	20	2.16	11.07
Sadah	21	10	12	8	9
Southern Red Sea	40	20	20	41.1	72.12
Najran	10	10	12	1.5	3
Sanaa	23	17	20	10	20
AlHodadah	20	[a]	[a]	6	29
Dhamar	22	20	[a]	12	12
Farasan	15	20	20	3.9	14
Zabid	21.5	[a]	[a]	5	32

Where [a] this city not included in the previous study

From these figures it is concluded that the values of the predominant period are varies greatly from one city to another depending on the type of underlying rocks or sediments. Also the maximum values of spectral acceleration are quite different for the area of study depending on many factors concerning with the seismic sources, path and local site characteristics. So, it is recommended that the detailed studies for the spectral accelerations and site response are necessary needed at each city and the results should take into consideration in the design of strategic buildings and developmental projects at each site.

Conclusions

The presence of the economic and heavy populated cities close to the earthquake belts of the Red Sea and southern Arabian Shield and due to the scarcity of strong earthquakes lead to increasing the seismic hazard potentialities for strategic buildings (e.g. dams, power plants) within these cities. So, this study depends on the available geological, geophysical and seismological data to assess the seismic hazard for the area. The area characterized by complicated geological structures due to the tectonic movements and volcanic eruptions accompanied with the Red Sea and later. This is indicated in the presence of various topographic features in Saudi Arabia and the Northern Yemen. From the distribution of both historical (200–1964) and instrumental (1964–2005) earthquakes, it is noticed that there are more than five hundreds of earthquakes have occurred in the area. Their magnitudes range from $2 \leq M \leq 8.0$. Most of earthquakes are epicentred along the transform faults of the southern Red Sea and southern Arabian Shield. The seismological catalogue is completed for earthquakes with magnitude less than 3 from 2001. About 218 earthquakes have relocated using more recent crustal structure models to enhance their location. Depending on these data there are four seismic source zones have defined for the area and these are; Sanaa-Dhamar zone; Southern Red Sea zone; Northern Yemen and Middle of Red Sea source zone.

From the recurrence study of earthquakes, it is found that the b value for the southern part of Arabian Shield is relatively high (1.06) compared with b values in the southern Red Sea ($b = 0.57–0.88$) which reflects the heterogeneity of the crust. Due to the separation of Arabian plate from the African one in the northeastern direction, the earthquakes that occurred along the Red Sea are of normal fault type from the location of their epicenters on the axial trough. On the other hand, the presence of transform faults bisected the Red Sea with NE–SW directions confirm the presence of some earthquakes with transform focal mechanism. The focal mechanisms of the recent earthquakes confirm that most of earthquakes in the southern Red Sea represent the strike-slip movements trending NE–SW. While the earthquakes on the land in the southern Arabian Shield occurred as a result of the vertical movement trending NW parallel to the axis of the Red Sea.

The seismic hazard assessment for the area in terms of Peak Ground Acceleration (PGA) time history and the calculation of response spectra was done using stochastic method. The results show that the value of PGA is different from one city to another one. PGA value for the bedrock at Yarim and Dhamar cities is about 12 cm/sec^2, 6 cm/sec^2 at Al-Hodadah, 5 cm/sec^2 at Zabid, 3.9 cm/sec^2 at Farasan, 1.5 cm/sec^2 at Najran, 8 cm/sec^2 at Sadah, 2.16 cm/sec^2 at Jizan and 0.67 cm/sec^2 at Abha city. The values of PGA is

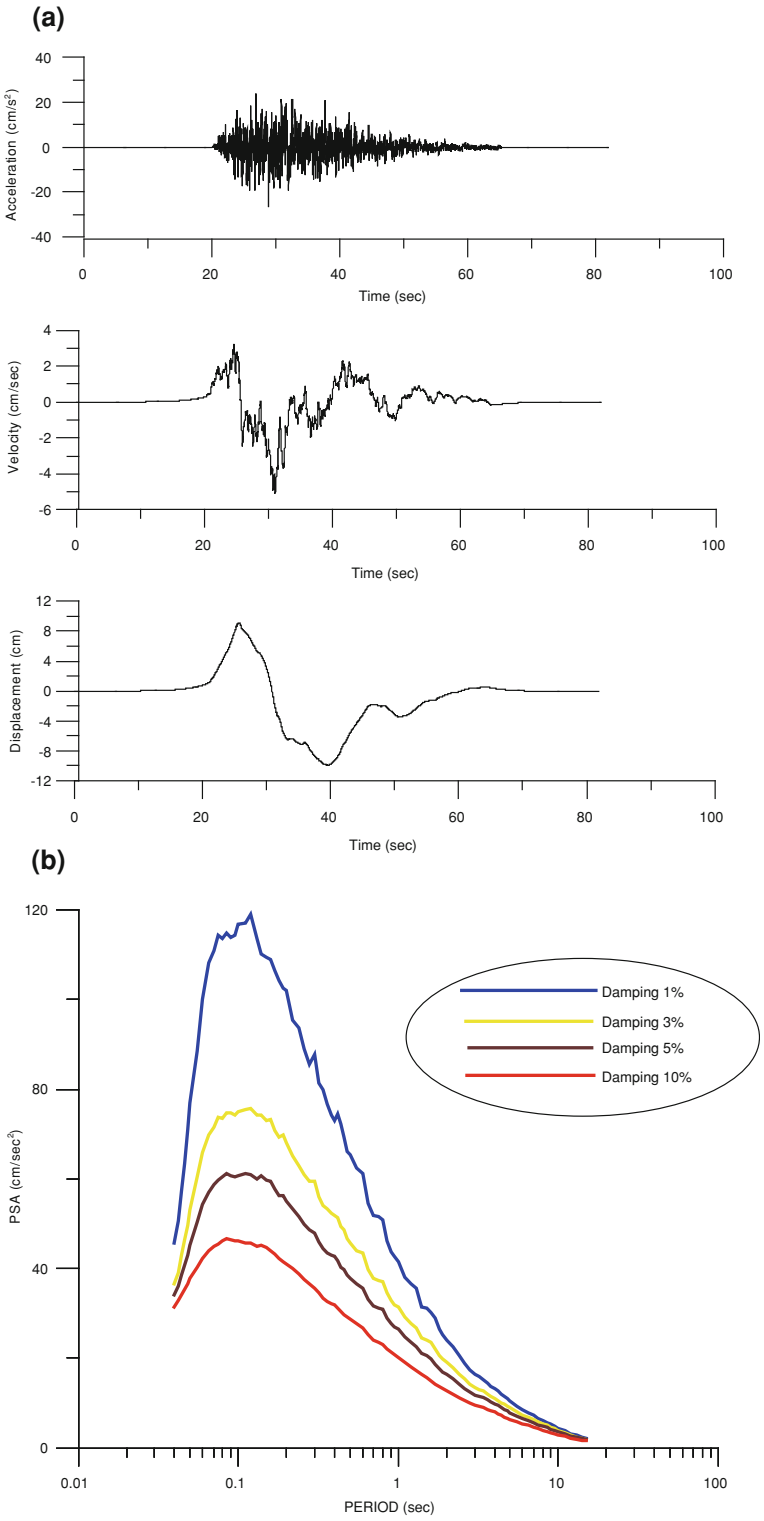

Fig. 16.10 **a** Simulated time history of PGA, velocity and displacement at Sana'a area in Quaternary rocks and **b** the response spectra at Sana'a with maximum PGA resulted in zone *1*

affected by the local soil sediments on the ground surface where PGA value is 32 cm/sec^2, 29 cm/sec^2, 14 cm/sec^2, 11.7 cm/sec^2 at Zabid, Al-Hodadah, Farasan, and Jizan respectively. There is no effect at the other cities due to their location on the basement rocks. Abha city can be affected where the value of PGA is about 39 cm/sec^2 due to the amplification effect of soft sediments of soil. The seismic hazard potentialities increase in the southwest of Arabian Shield close to Zabid area due to the amplification of soft soil sediments. Also the hazard potentialities for the southern Red

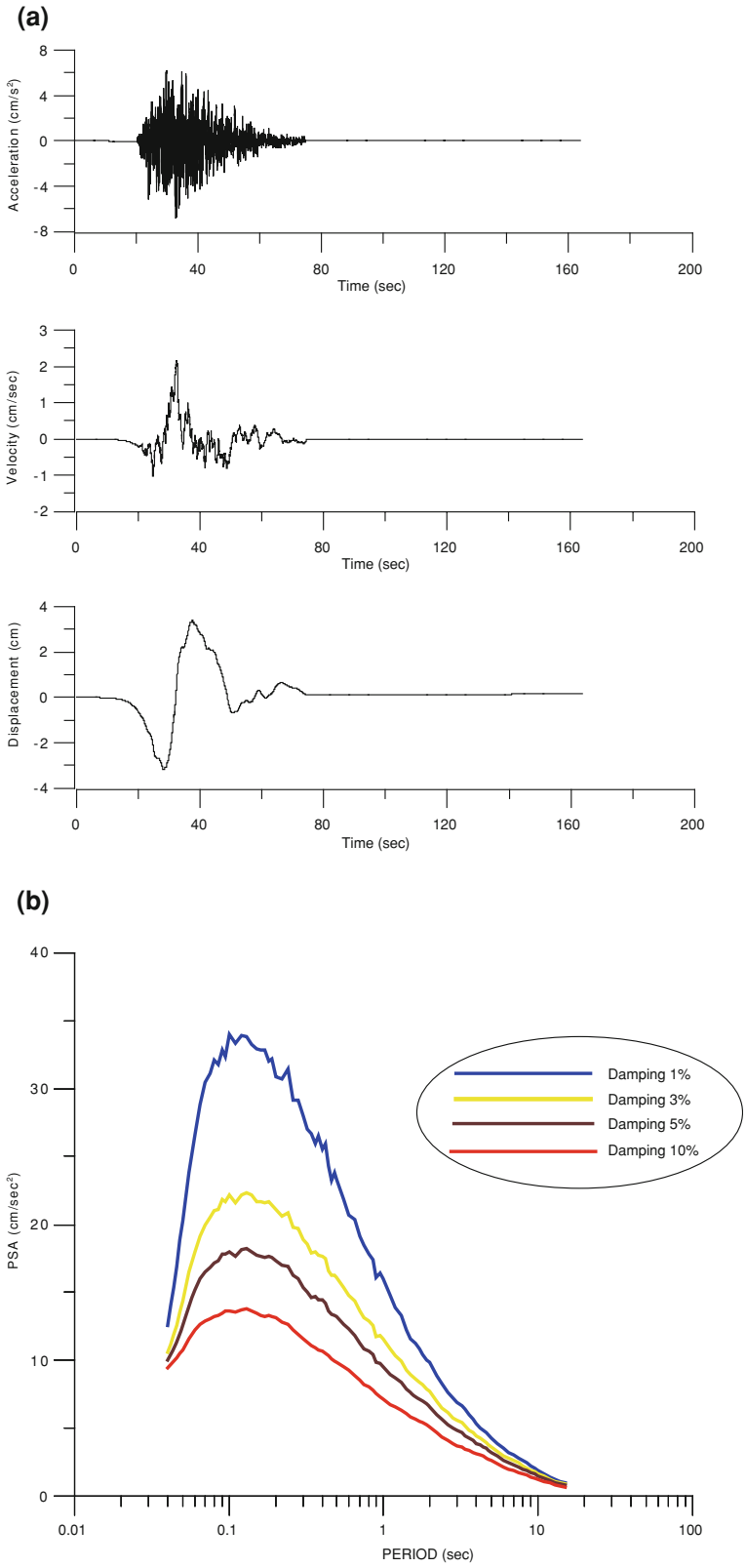

Fig. 16.11 **a** Simulated time history of PGA, velocity and displacement at Dhamar area in Permian rocks and **b** the response spectra at Dhamar with maximum PGA resulted in zone *1*

Sea are relatively high but the presence of the oceanic crust and salt structures may attenuate the seismic waves. The difference in PGA values this study and the previous studies refers mainly to the shortage period of earthquake observation in Saudi Arabia (1964 to 2005), and then the present method of treatment is more reliable than the previous ones.

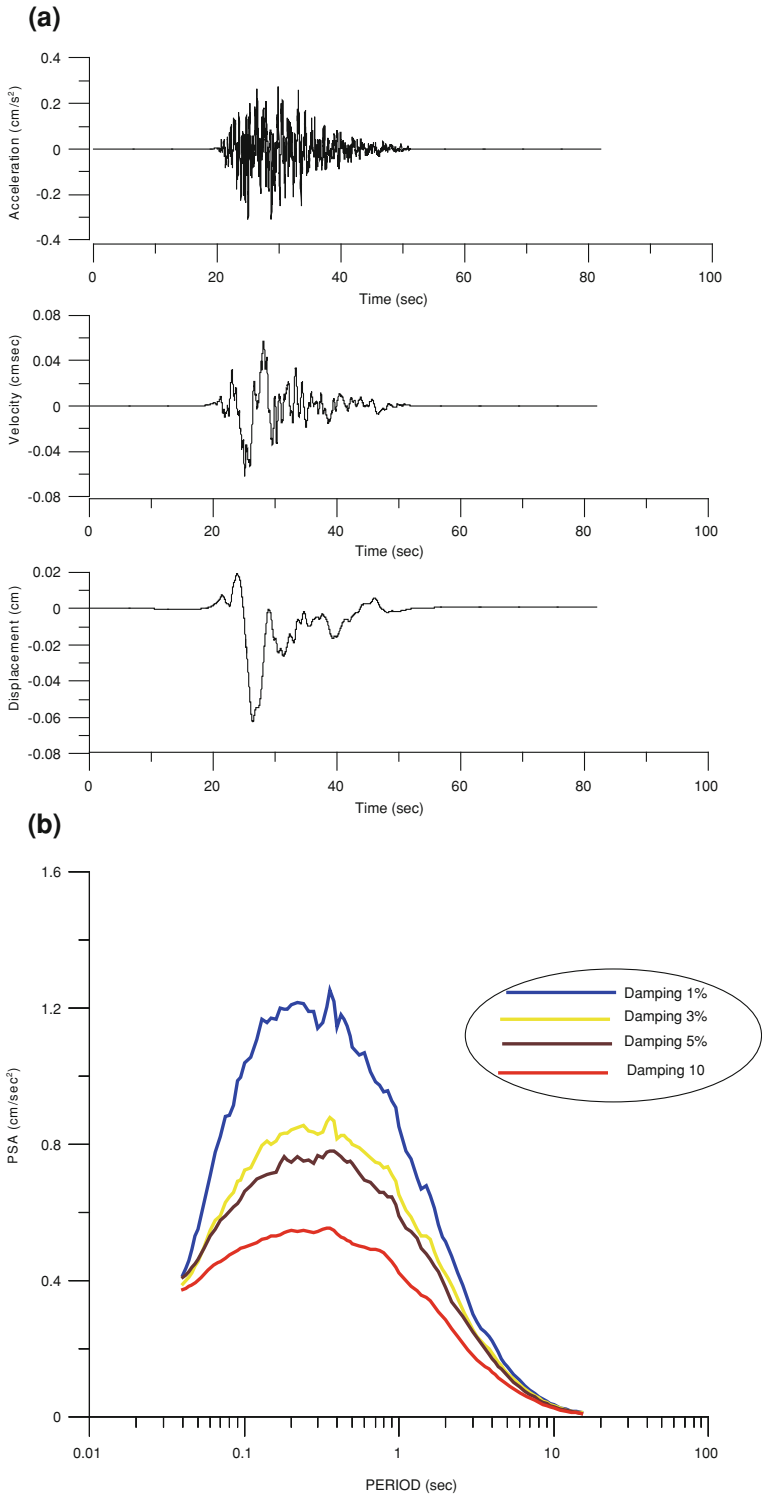

Fig. 16.12 **a** Simulated time history of PGA, velocity and displacement at Abha area in Pre-Cambrian rocks and **b** the response spectra at Abha with maximum PGA resulted in zone *4*

Response spectra for different rock units at the big cities within the area were calculated with 1, 3, 5 and 10 % of critical damping. The results show that the highest value of PGA simulated at Sanaa and Al-Hodadah is 120 cm/sec^2 with 1 % of critical damping. It is noticed that the amplification of Quaternary rocks should be taken into consideration in the design of strategic projects and buildings.

Acknowledgements The authors would like to express their thanks and deep gratitude to all staff of KSU and KACST seismic center for their kind support and valuable discussion.

References

Abdel-Gawad M (1969) New evidence of transcurrent movements in the Red Sea area and Petroleum implications. Am Assoc Petrol Geol Bull 53(7):1466–1479

AL-Amri AM (1994) Seismicity of the south-western region of the Arabian Shield and southern Red Sea, department of geology, King Saud University. J Afr Earth Sci 19(1):17–25

Al-Amri AM (1995) Preliminary seismic hazard assessment of the southern Red Sea region. European earthquake engineering, pp 33–38

Al-Amri AM (1998) The crustal structure of the Western Arabian platform from the spectral analysis of long-period P-wave amplitude ratios. Tectonophysics 290:271–283

Al- Amri AM, Punsalan BT, Uy E A (1998) Spatial distribution of the seismicity parameter in the Red Sea reigions. J Earth Sci 16(5–6):557–563

Al-Amri A, Alkhalifah T (2004) Improving the level of seismic hazard parameters in Saudi Arabia using earthquake location and magnitude calibration. Project no. 20–68, King Abdul Aziz City for Science & Technology, Riyadh

AL-Haddad M, Siddiqi GH, AL-Zaid R, Arafah A, Necioglu A, Turkelli N (1994) A basis for evaluation of seismic hazard and design for Saudi Arabia. Earthq Spectra 10(2):231–258

Alsinawi SA (1983) Dhamar earthquake of 13/12/82 a report submitted to the Yemeni Government, p 34 (Arabic text)

Alsinawi SA (1986) Historical seismicity of the Arab region. Proceedings of the third Arab seismological seminar, Riyadh Saudi Arabia, pp 11–33

Ambraseys NN (1988) The seismicity of Saudi Arabia and adjacent area, Report Prepared for the Kingdom of Saudi Arabia. ESEE, Imperial Col Sci Tech London, U.K. Report 88/11. p 294

Ambraseys NN, Melville CP (1983) Seismicity of Yemen. Nature 303:321–323

Ambraseys NN, Melville CP, Adams RD (1994) The seismicity of Egypt, Arabia and the Red Sea- ahistorical review. Cambridge University Press and King Abdul Aziz City for Science and Technology, p 181

Atkinson GM, Boore DM (1995) Ground motion relations for eastern North America. Bull Seism Soc Am 85:17–30

Barazangi M (1981) Evaluation of Seismic Risk along the western part of the Arabian plate: discussion and recommendations, Bull Fac Earth Sci K.A.U pp 77–87

Boore DM, Atkinson GM (1987) Stochastic prediction of ground motion and spectral response parameters at hard-rock sites in eastern North America. Bull Seism Soc Am 77:440–467

Boore DM (1983) Stochastic simulation of high frequency ground motions based on seismological models of the radiated spectra. Bull Seism Soc Am 73:1865–1894

Boore DM (1996) SMSIM- Fortran programs for simulating OFR 96-80-A, USGS, Open-File Report 00-509, p 55

Boore DM (2002) SMSIM: Stochastic method simulation of ground motion from earthquakes. In: Lee WHK, Kanamorri H, Jennings PC, Kisslinger DC (eds) International handbook of earthquake and engineering seismology, Chapter 85.13, Academic, London

Brown GF, Jackson RO, Bogue RG, Maclean WH (1963) Geologic map of the Southern Hijaz quadrangle, Kingdom of Saudi Arabia: U.S. Geol. Survey Misc Geol Inv Map I-210A, scale 1:500000

Drake CL, Girdler RW (1964) A geophysical study of the Red Sea. Royal Astron Soc Geophys J 8:473–495

El-Difrway MFI (1996) Earthquake ground motion amplification in the greater Cairo area. Bull Fac Sci Cairo Univ Vol 63:105–132

El-Isa Z, Al- Shanti A (1989) Seismicity and tectonics of the Red Sea and Western Arabia. Geophys J R Astron Soc 97:449–457

Fairhead JD (1968) The seismicity of East African rift system 1955–1968, MSc Dissertation, University of Newcastle upon Tyne

Fairhead JD, Girdler R (1970) The seismicity of the Red Sea, Gulf of Aden and Afar triangle. Phis Trans R Soc Lond A 267:49–74

Fairhead JD, Girdler R (1972) The seismicity of East African rift system. Tectonophysics 15:115–122

Gutenberg GB, Richter C (1944) The seismicity of the earth and associated phenomena. Hafner Publishing Co., New York, p 310

Hanks TC (1982) Fmax. Bull Seism Soc Am 72:1867–1879

Hanks TC, McGuire RK (1981) The character of high frequency strong ground motion. Bull Seism Soc Am 71:2071–2095

Hatzdimitrio P, Papadimitio E, Mountrakis D, Papazachos B (1985) The seismic parameter b of the frequency-magnitude relation and its association with the geological zones in the area of Greece. Tectonophysics 120:141–151

Isacks B, Oliver J (1964) Seismic waves with frequencies from 1 to 100 cycles per second recorded in a deep mine in northern New Jersey. Bull Seismol Soc Am 54:1941–1979

Karnik V (1969) Seismicity of the European area. D. Reidel, Dordrecht, p 364, Part I

Langer CJ, Bollinger GA, Merghelani HM (1987) Aftershocks of the 13 December 1982 North Yemen Earthquake: Conjugate normal faulting in an extensional setting. Bull Seismol Soc Am 77(6):2038–2055

Makris J, Berendsen D, Denecke C (1986) Sonne cruise no. 29 in the central Red Sea Tech Rept, Project No. R 341, IfG Hamgurg, p 34

Makris J, Bobsien M, Meier K, Rihm R (1989) Sonne cruise no. 53 in the southern Red Sea. Tech Rept, Project No. R 383 B6, IfG Hamburg, p 83

McKenze D, Davis D, Molnar P (1970) Plate tectonics of the Red Sea and east Africa. Nature 226:243–248

Midorikawa S (1987) Prediction of isoseismal map in the Kanto plain due to hypothetical earthquake. J Struct Eng 33:43–48

Mogi K (1962) Study of the elastic shocks caused by the fracture of heterogeneous materials and its relations to earthquake phenomena. Bull Earth Res Inst 40:125–173

Mountrakis D, Sapountzis E, Kilias A, Elefteriadis G, Christophides G (1983) Paleogeographic conditions in the western Pelagonian margin in Greece during the intial rifting of the continental area. Can J Earth Sci 20:1673–1681

Nuttli O, Herrmann R (1984) Ground motion of Mississippi Valley earthquakes. Tech J Topics Civil Eng 110:54–69

Papazachos BC (1980) Seismicity rates and long-term earthquake prediction in the Agean area. Quaterniones Geodaesiae 3:171–190

Papazachos BC, Kiratzi AA, Hatzidimitriou PM, Rocca ACh (1984) Seismic faults in the Agean area. Tectonophysics 106:71–85

Papazachos BC, Scordilis EM, Papagiotopoulos DG, Papazachos CB, Karakaisis GF (2004) Global relations between seismic fault parameters and moment magnitude of earthquakes. Bull Geol Soc Greece XXXVI:1482–1489

Poirier JP, Taher MA (1980) Historical seismicity in the near and middle east, North Africa and Spain from Arabic documents (VIIth–Xviith century). Bull Seism Soc Amer 70(6):2185–2201

Powers R, Ramierez L, Redmond C, Elberg E (1966) Geology of the Arabian Peninsula: sedimentary geology of Saudi Arabia, US Geol. Surv Prof Paper, 560-D, p 147

Reiter L (1991) Earthquakes hazard analysis. Colombia Univ Press, New York

Thenhaus PC (1983) Summary of workshop concerning regional seismic zones of parts of the United States, by the U.S. Geological Survey, 865, p 36

Thenhaus PC, Algermissen S, Perkins D, Hansen S, Diment W (1986) Probabilistic estimates of the seismic ground-motion hazards in western Saudi Arabia, U.S. Geological Surv Bull No. 1968, p 40